

Long-term α - and spontaneous fission measurement of a Rf/Db sample chemically prepared in a ^{48}Ca on ^{243}Am experiment

Rugard Dressler, Robert Eichler, and Dorothea Schumann

Laboratory for Radiochemistry and Environmental Chemistry, Paul Scherrer Institut, Switzerland

Sergey Shishkin

JINR, Flerov Laboratory of Nuclear Reactions, RU-141980 Dubna, Russia

(Received 24 September 2008; revised manuscript received 5 February 2009; published 8 May 2009)

Results from long-term measurements of a chemically separated Db/Rf sample prepared from the products of a ^{48}Ca on ^{243}Am irradiation are presented. The sample with the highest spontaneous fission activity out of eight samples produced in the course of chemical experiments performed in 2004 was selected for these measurements. We conclude that there is no evidence for SF-decay originating from heavy actinide isotopes in this sample. Hence, it is appropriate to assign the SF-events observed in this experiment to decay products of $^{288}115$.

DOI: [10.1103/PhysRevC.79.054605](https://doi.org/10.1103/PhysRevC.79.054605)

PACS number(s): 27.90.+b, 23.60.+e, 25.85.Ca, 25.70.Hi

I. INTRODUCTION

The discovery of relatively long-lived isotopes of transactinides in so-called “warm” fusion reactions using ^{48}Ca beams and actinide targets (see, e.g., [1]) was one of the most important steps toward the “Island of Stability” of superheavy elements (SHE) within the last 20 years. The isotopes produced so far show an enhanced stability approaching $Z = 114$ $N = 184$, as predicted about 40 years ago [2–6]. These results open up new possibilities not only for the physics of superheavy elements but also for their chemical investigations.

In 2003, the Dubna Gas-Filled Recoil Separator (DGFRS) group at the Flerov Laboratory of Nuclear Reactions (FLNR) Dubna reported the observation of three decay chains related to element 115 [7] using the nuclear fusion reaction of ^{48}Ca on ^{243}Am . Five consecutive α -decays, assigned to the decays of $^{288}115$, $^{284}113$, $^{280}111$, ^{276}Mt , and ^{272}Bh , followed by a spontaneous fission (SF) event assigned to ^{268}Db were detected [7]. In a second experiment in 2004, the chemical identification of the long-lived SF-decaying descendants confirmed the production of $^{288}115$ in this nuclear reaction [8]. A rotating target of ^{243}Am (99.9% purity, 1.2 mg/cm² surface density) deposited onto a Ti backing foil (1.5 μm thickness) was irradiated with a ^{48}Ca beam. The beam energy in the center of the target was 247 MeV. The reaction products recoiled out of the target and were implanted in a Cu block (100 mm distance from the target, 50 mm diameter). After the irradiation period (between 20 h and 48 h) the uppermost 7–10 μm of the Cu catcher were planed down and the shavings were used for the chemical procedure to separate a fraction containing group 4 and 5 elements. The finally obtained liquid fraction was transferred onto a polyethylene foil (0.4 μm thickness, 15 mm diameter). The SF-activity of these samples was measured for up to 957 h in a 4π -geometry using an event-by-event detection system. For more technical details regarding this experiment see [1, 8–10].

Fifteen SF-events were measured in the group 4 and 5 fraction of an aqueous chemical separation and assigned to the terminating decay product of $^{288}115$. Therefore, these

chemical investigations were used together with the first physical experiments to claim the discovery of element 115 and element 113 as its primary α -decay product [10].

Since the isotope ^{268}Db (or ^{268}Rf , if ^{268}Db undergoes electron-capture decay) can be detected via SF-measurements only, the chemical separation procedure has to guarantee a complete decontamination from heavy actinides produced in multinucleon transfer reactions at much higher production rates. This was achieved by a combined precipitation and ion exchange technique using an HF-containing aqueous solution. Unfortunately, the immediate α -measurement of the prepared samples was not able to exclude a contamination with heavy actinides due to the high content of projectile-like by-products. The main β -emitters in the final samples were isotopes produced in quasifission, fusion-fission or multinucleon transfer reactions. The produced Zr and Nb isotopes being members of group 4 and 5 cannot be depleted as a matter of principle. The produced Sc and Rh isotopes (observed were $^{47,48}\text{Sc}$ and $^{100,101m}\text{Rh}$) could be separated from the final samples only with a suppression factor of 1.5 and 33, respectively. Due to the high initial concentration, the remaining activity in the final sample was still relatively high. The high β -activity made the α -spectroscopic detection of actinide contaminations impossible. The γ -spectroscopic measurement of the final samples obtained during the experiment show a decontamination factor for lanthanides (homologous to heavy actinides) greater than 100, this number being limited by the detection method. A more significant decontamination factor of 10^5 was demonstrated in identical model experiments for lanthanum using the ICP-OES technique. These results, described in detail in [9], indicate an extremely small probability for an actinide contamination in the final samples, but still the direct proof that the measured Rf/Db fractions are sufficiently well separated from actinides was missing. Long-lived actinide isotopes (e.g., $^{248,250}\text{Cm}$, $^{250,252}\text{Cf}$) are still expected to be detectable after the decay of the disturbing β -activity assuming that the observed SF-events in the final sample originate mainly from heavy actinides.

Here, we present α - and SF-spectra of sample no. 4 (the numeration of samples as given in [8] is used). Sample no. 4 contained the highest SF-activity per beam dose within the experiment: three SF-events assigned to ^{268}Db or ^{268}Rf were registered during the first 96 h of measurement (starting 2 to 3 h after the end of bombardment) and no additional events in the second registration period of 262 h. This sample was selected as the most valuable candidate to prove the quality of the actinide separation.

II. EXPERIMENTAL DETAILS AND RESULTS

The nuclear reaction products collected on June 15, 2004 during a 22 h irradiation were used for preparation of sample no. 4. In total 2.9×10^{17} ^{48}Ca ions passed the 1.2 mg/cm^2 ^{243}Am target [8]. After the chemical treatments and preparation of the sample, a 4π -geometry measurement recording α - and SF-events as well as coincident neutrons was performed over 96 h. Afterwards (on June 19, 2004) the sample was transferred to a similar counting system recording α - and SF-events for an additional 262 h. In both measurement setups the efficiency to register α -particles or SF fragments was 72%. For additional experimental details see [7–10].

The long-term α -spectroscopic measurement of sample no. 4 was started about two years after its preparation on May 5, 2006. A 2π geometry setup with a 600 mm^2 PIPS α -detector (2 mm distance between sample and detector surface, i.e., 42.8% detection efficiency) was used for a 348 h measurement. The detector was slightly contaminated with ^{239}Pu , ^{241}Am , and ^{244}Cm from standard calibration sources. Additionally, the entire detector chamber was contaminated with ^{236}Pu and/or ^{232}U from previous measurements. The contaminants are visible in the spectra of a 100 h background measurement shown in Fig. 1 (blue line). Besides these contaminations, the spectrum of the 348 h measurement (Fig. 1, red bars) contains traces of the sputtered target material ^{243}Am and target like transfer products ^{237}Np , $^{238-242}\text{Pu}$, $^{243,244}\text{Cm}$ as well as light transfer products $^{208,210}\text{Po}$. The main part of the $^{236}\text{Pu}/^{232}\text{U}$ contamination is not visible in this spectrum due to the shielding of the active detector surface by the sample carrier.

^{216}Po , ^{212}Bi , and ^{212}Po are still detectable due to the transport of ^{220}Rn emanation to the detector surfaces. The energy calibration of this setup was performed using the α -spectra recorded in the background measurement. No α -lines of heavy actinides (e.g., ^{252}Es , ^{252}Cf) could be identified.

The SF-activity was measured in a second setup (started on July 4, 2006) using an uncontaminated counting chamber and a new set of two PIPS-detectors (300 mm^2) in 4π counting geometry (3 mm distance between the detector surfaces, i.e., 84.8% detection efficiency) for 3600 h. The energy calibration of this setup was done after finishing this measurement using a mixed α -source (^{148}Gd and ^{244}Cm). The capability of the setup to detect SF-fragments was proven in a separate measurement. A ^{252}Cf source covered with a $30 \text{ }\mu\text{g/cm}^2$ polyethylene foil was measured in front of a structurally identical PIPS detector (2π geometry). The measured SF-fragment energy distribution shows an energetic shift of 22.5 MeV in direction to lower energies compared with the established values of 80.3 MeV of the heavier SF-fragments and 106.2 MeV of the lighter SF-fragments [11]. This shift originates from differences in pulse height defects of the used detectors and from energy losses in the polyethylene coverage of the SF-source. A similar shift is expected for a comparison with the high energy values given in [7,8].

No coincident high energetic events were recorded during this measurement. Thirteen single events were detected in the energy range from 15 MeV to 40 MeV, which are attributed to high energetic cosmic background. The sum-spectra of both detectors together with the sum of the normalized measured SF-fragment energy distribution of ^{252}Cf are shown in Fig. 2. The previously measured six SF fragments of the recorded three coincident SF-events attributed to ^{268}Db from sample no. 4 are also indicated (red bars).

III. DISCUSSION

The upper limit of the SF-rate originating from heavy actinides can be estimated in two independent ways using the long-term SF-measurement as well as the α -measurement. The counting period of the SF measurement of sample no. 4 in [8]

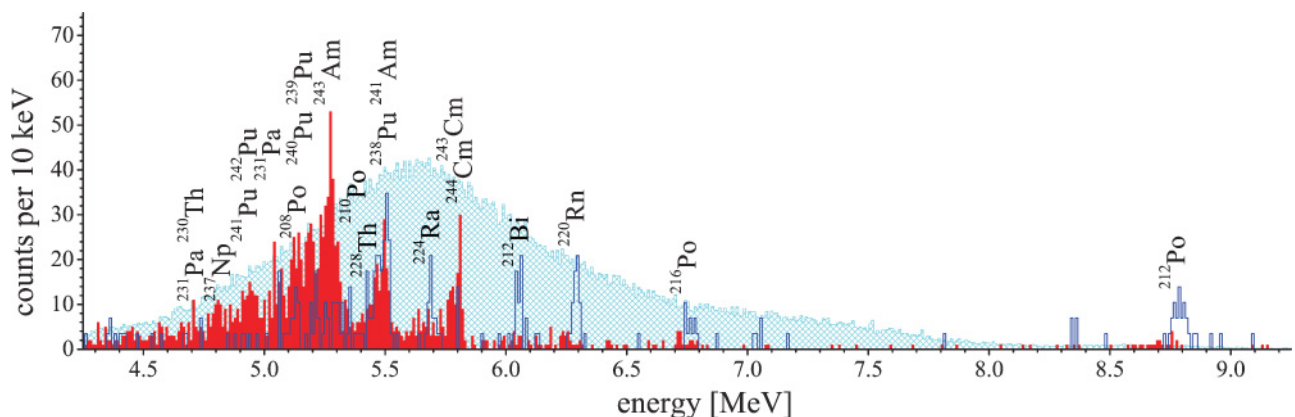


FIG. 1. (Color online) α -spectrum of sample no. 4: originally measured for 96 h (cyan hatched, scaled 1:20); measured for 348 h (red bars); and the 100 h blank-spectrum (detector contamination) scaled to the same measurement time (blue line).

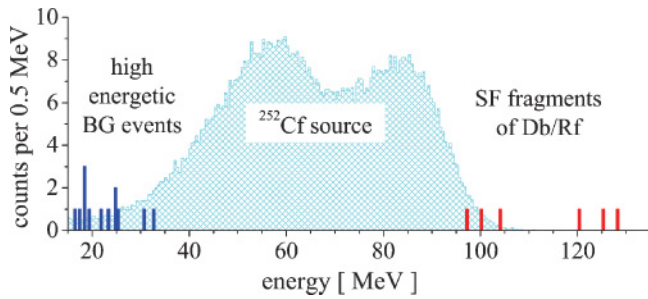


FIG. 2. (Color online) SF-spectra of sample no. 4 measured in 4π counting geometry: originally coincident measured SF-events (red) [8]; high energetic events measured in this work during 3600 h (blue); ^{252}Cf calibration spectrum measured in 2π geometry (cyan, scaled 1:100).

was split into two parts. The first 96 h counting period (containing the three SF-events) was considered as the SF-measurement of the Db/Rf content. The remaining second counting interval of 262 h was used as the first part of the long-term SF-measurement in the following analysis. Thus, the heavy actinides content of sample no. 4 was overall measured during 3862 h. No additional SF-event was observed during this measurement. The upper limit of the SF-rate can be deduced as 7.8×10^{-4} SF-events per hour (95.45% c.i.) originating from long-lived heavy actinides decay. Therefore, within the first 96 h measurement period the probability to detect one, two, or three SF-events originating from these isotopes will be less than 6.9%, 0.26%, or $6.4 \times 10^{-3}\%$, respectively.

The measurement of the α -decay of actinides in sample no. 4 opens up a more sensitive possibility to determine the amount of disturbing heavy actinides. For that purpose, the knowledge of the multinucleon transfer cross section in the reaction ^{48}Ca on ^{243}Am is required to estimate the

production of all SF-decaying actinides. Unfortunately, such experimental data are not available. However, it is well known that multinucleon transfer cross sections are not very sensitive to small variations of the proton or neutron number of the target nuclide (see [12–21]). We used the experimentally known multinucleon transfer cross sections of ^{48}Ca on ^{248}Cm at similar beam energies to estimate the production cross sections for the relevant actinide isotopes in the ^{48}Ca on ^{243}Am reaction. These experimental data were taken from [16] for the heavier reaction products (beam energy 246–259 MeV) and from [22] for the lighter reaction products (beam energy 248–263 MeV). We assumed that the multinucleon transfer cross sections depend only on the number of exchanged nucleons. Therefore, the multinucleon transfer cross sections of ^{48}Ca on ^{243}Am can be estimated from the corresponding reaction channels in the reaction of ^{48}Ca and ^{248}Cm . Unfortunately, this approach yields only a few of the cross sections of the isotopes under discussion directly. Different extrapolation procedures were used to cover the entire region of heavy actinide isotopes in this paper. In Fig. 3 a rough estimate of the isotopic cross section landscape in the N - Z -plane of the reaction ^{48}Ca on ^{248}Cm is depicted. We used the kriging-interpolation method [23,24] to visualize the given data in a two dimensional contour plot. This method gives the best linear unbiased estimator for optimal predictions of unknown values from data observed at known locations. We added three grid points at ^{246}At , ^{228}Rf , and ^{265}Rf with an arbitrarily chosen value of $\sigma = 10^{-60}$ b to extend this visualization over the whole range of actinides. It is obvious that the maximum of the multinucleon transfer cross section is located close to the target isotope as expected and that for lighter isotopes a saddle point in the vicinity of ^{231}Pa appears. The kriging method should only serve as a visualization tool for the cross section landscape outside the experimentally known

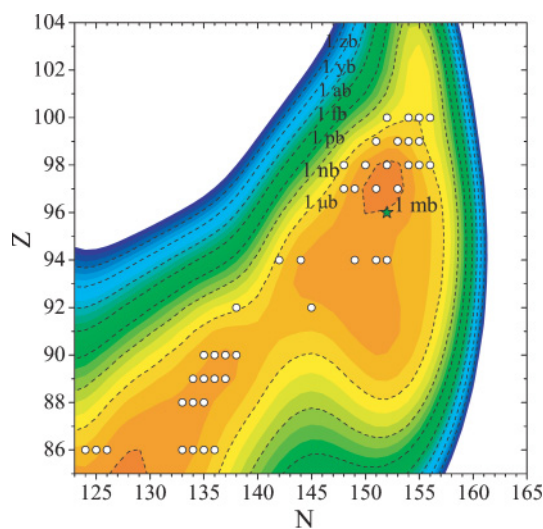


FIG. 3. (Color online) Cross section landscape of multinucleon transfer reactions of ^{48}Ca on ^{248}Cm at 247 MeV projectile energy. Experimental data points taken from [16,22] are indicated by open circles, the target isotope is indicated by a green star. The contour lines are calculated using the kriging algorithm [23,24].

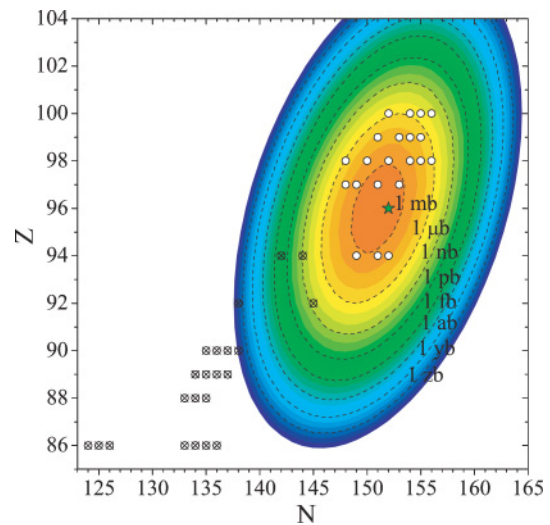


FIG. 4. (Color online) Cross section landscape of multinucleon transfer reactions of ^{48}Ca on ^{248}Cm at 247 MeV projectile energy. Experimental data points are taken from [16,22]. The data points used for the fit with Eqs. (1) are indicated by open circles, not used data points are crossed through. The target isotope is indicated by a green star.

region. It cannot be used for an extrapolation of cross sections far away from the experimental data.

Two other models were used to extrapolate the known cross sections into the most interesting region. The first method was proposed by Breuer *et al.* [13,25] to investigate the charge and mass distribution in ^{56}Fe induced reactions of the projectile like reaction products. A parametrization of the cross sections landscape can be obtained by a two dimensional gaussian fit. For symmetric reasons this method will also work for the complementary target-like reaction products. Unfortunately, no data points are available in the vicinity of the target isotope. Most of the lighter target-like reaction products measured in [22] are too far beyond the saddle point to be well described by this model (see Fig. 3). Only the isotopes $^{243,245,246}\text{Pu}$ can be included as representatives for lighter transfer products. To perform the fit, we slightly adapted the equations given in [13], as shown in Eqs. (1).

The resulting cross section landscape is depicted in Fig. 4, where the obtained parameters are $\sigma_0 = 9.00 \pm 0.18$, $s_Z = 0.866 \pm 0.018$, $s_N = 1.151 \pm 0.029$, and $s_{NZ} = -1.250 \pm 0.074$, respectively (all errors are given as 95.45% c.i.). The parameters $\bar{Z} = 96$ and $\bar{N} = 151$ were kept fixed after the first fitting iterations to avoid fractional nucleon numbers. A reduced χ^2 of 0.785 for the logarithm of the cross sections was obtained,

$$\ln\left(\frac{\sigma_{\text{Breuer}}(\Delta N, \Delta Z)}{1\mu\text{b}}\right) \quad (1a)$$

$$= \sigma_0 - \frac{1}{2} \left\{ \left(\frac{\Delta Z}{s_Z}\right)^2 + \left(\frac{\Delta N}{s_N}\right)^2 + \frac{\Delta Z \Delta}{s_{NZ}} \right\},$$

$$\Delta Z = Z - \bar{Z}, \quad \Delta N = N - \bar{N}. \quad (1b)$$

The fitted cross section values σ_{Breuer} and their relative deviations from the experimental data are compiled in Table I. The values are in reasonable agreement with the experimental data, with exception of the Es isotopes and ^{252}Fm , where the cross sections are significantly overestimated by this method. Additionally, the model underestimates the transfer cross sections for Fm isotopes heavier than 254 as well as for all isotopes of elements heavier than Fm in a systematic way.

Figure 5 presents the estimated cross section landscape of the target-like multinucleon transfer products of ^{48}Ca on ^{243}Am . We assume that in general these cross sections should be larger than the cross sections for the formation of compound nuclei. In the reaction $^{243}\text{Am}(^{48}\text{Ca}; 3n)^{288}\text{115}$ a value of $\sigma = 2.7_{-1.6}^{+4.8}$ pb was deduced in [10]. Therefore, estimated cross sections of less than a few fb for Md isotopes are unrealistic. We conclude that the obtained parametrization cannot be used to estimate the production rate of the heaviest actinides.

A second model proposed by [26] was evaluated. In a first step the isotopic cross sections and in a second step the quadratic dependence of the obtained fit parameters on the atomic number were fitted. The resulting fit equations are given in Eqs. (2). Equation (2a) was applied with fixed ΔZ to the experimental data of [16] to determine the values

TABLE I. Comparison of experimental multinucleon transfer cross sections of the reaction ^{48}Ca on ^{248}Cm at an excitation energy of 246–259 MeV with different fit models (for details see text).

	σ_{exp}^a [μb]	s_{rel}^b [%]	σ_{Breuer}^c [μb]	$\Delta\sigma_{\text{rel}}^d$ [%]	σ_{calc}^e [μb]	$\Delta\sigma_{\text{rel}}^d$ [%]
^{245}Bk	40	50	42	4.5	51	26
^{246}Bk	360	22	412	14	347	-3.4
^{248m}Bk	2900	18	4150	43	2950	1.8
^{250}Bk	2520	17	2040	-19	2540	0.88
^{246}Cf	1.8	14	1.7	-5.2	1.40	-22
^{248}Cf	260	14	173	-33	210	-19
^{250}Cf	2380	19	858	-64	1020	-57
^{252}Cf	225	16	208	-7.7	160	-29
^{253}Cf	12	32	33	174	18	45
^{254}Cf	1.5	42	2.5	63	0.81	-46
^{250}Es	6.6	52	20	204	16	139
^{252}Es	30	27	49	63	60	100
^{253}Es	10	22	25	146	30	187
^{254m}Es	2.0	27	5.8	191	5.4	169
^{252}Fm	0.11	47	0.64	485	0.106	-3.4
^{254}Fm	0.81	17	0.77	-4.7	0.803	-0.85
^{255}Fm	0.9	42	0.27	-70	0.66	-27
^{256}Fm	0.24	32	0.045	-81	0.241	0.37

^aCross section values taken from [16].

^bThe total standard deviation of absolute cross sections was calculated using the data given in Table II column five of [16] taking into account the given additional systematic error of 12%.

^cEstimated cross section using Eqs. (1). Fitting parameters are given in text.

^dRelative deviation of calculated cross section from experimental value. $\Delta\sigma_{\text{rel}} = \frac{\sigma_{\text{calc}}}{\sigma_{\text{exp}}} - 1$

^eEstimated cross section using Eqs. (2). Fitting parameters are given in Table II.

of the parameters P_i in dependence of the neutron number. Subsequently, the parameters P_i are used as input for Eq. (2b) to establish an additional dependence of the proton number. The resulting parameter set $\alpha_{i,j}$ is given in Table II. In this case a reduced χ^2 of 0.550 for the logarithm of the cross sections was obtained,

$$\ln\left(\frac{\sigma_{\text{calc}}(\Delta N, \Delta Z)}{1\mu\text{b}}\right) = P_1(\Delta Z)(P_2(\Delta Z) - \Delta N)^2 + P_3(\Delta Z), \quad (2a)$$

$$P_i(\Delta Z) = \alpha_{i,1}(\alpha_{i,2} - \Delta Z)^2 + \alpha_{i,3}. \quad (2b)$$

TABLE II. Parameter set to fit multinucleon transfer cross sections of ^{48}Ca on ^{248}Cm using Eqs. (2). (The 95.45% uncertainties of the $\alpha_{i,j}$ parameters are given.)

$i \setminus j$	$j = 1$	$j = 2$	$j = 3$
$i = 1$	1.43 ± 0.10	0.373 ± 0.036	-0.201 ± 0.038
$i = 2$	2.877 ± 0.018	0.0519 ± 0.0010	-0.4688 ± 0.0018
$i = 3$	0.66 ± 1.18	-0.76 ± 0.48	8.29 ± 0.74

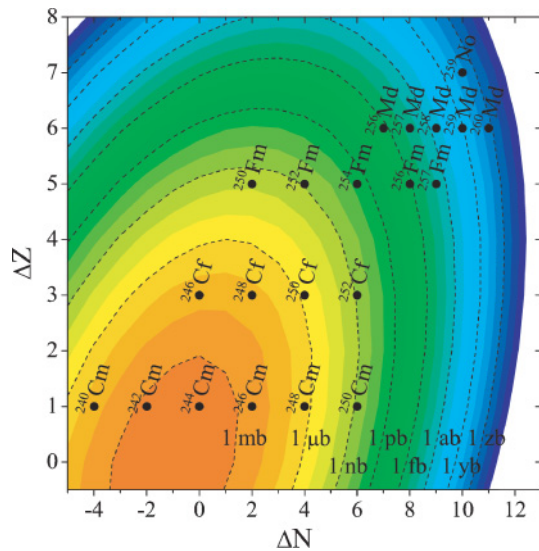


FIG. 5. (Color online) Cross section landscape of multinucleon transfer reactions of ^{48}Ca on ^{243}Am at 247 MeV projectile energy calculated with Eqs. (1). The isotopes which are possible main sources of SF-events are depicted.

In Table I the extrapolated values σ_{calc} are included in columns six and seven. For all measured isotopes the transfer cross sections are evidently reproduced within an uncertainty of about $\pm 60\%$. The only exception are Es isotopes, where the cross sections are overestimated by a factor between two and three. We conclude that the fit using Eqs. (2) follows better the experimental data than the fit using Eqs. (1). This is mainly due to the larger number of free parameters in the second approach. We used this parametrization to estimate the production rate of the heaviest actinides. In Fig. 6 the estimated cross section landscape of the target-like multinucleon transfer products of ^{48}Ca on ^{243}Am is depicted. The region of physically meaningful values is framed by dash-dotted lines. On one side this region is limited by the target element and on the other side by the minimum of isotonic cross sections of ^{246}Fm , ^{252}Md , and ^{258}No , respectively.

Using these results a more significant estimation of the SF contribution originating from nuclear transfer products in the heavy actinide region can be deduced. For this purpose the following isotopes were taken into consideration: $^{240,242-246,248,250}\text{Cm}$, $^{242-249}\text{Bk}$, $^{246,248-250,252-256}\text{Cf}$, $^{246,248,250,252-256}\text{Es}$, $^{250,252-257}\text{Fm}$, $^{254-260}\text{Md}$, $^{254-257,259}\text{No}$. Both the contribution due to direct production of these isotopes and the indirect production due to the radioactive decay were taken into account.

The content of actinides in the final sample can not be simply estimated using the beam dose, the target thickness, and the cross sections. This number will be essentially reduced due to the kinematical as well as chemical separation of

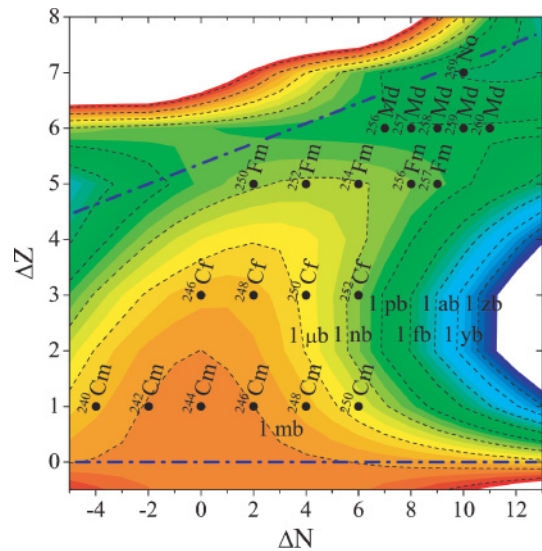


FIG. 6. (Color online) Cross section landscape of multinucleon transfer reactions of ^{48}Ca on ^{243}Am at 247 MeV projectile energy calculated with Eqs. (2). The dash-dotted blue lines mark the region of physically meaningful extrapolations. The isotopes which are possible main sources of SF-events are depicted.

actinides during the production and sample preparation. However, assuming that all actinides behave similar under the experimental conditions, the isotopic ratios will be conserved. Therefore, the number of SF-events during the first measurement period can be estimated from the number of observed ^{243}Cm and ^{244}Cm decays during the long-term α -measurement and the above deduced production cross sections. In total 105 α -events between 5.72 MeV and 5.84 MeV were attributed to the decay of ^{243}Cm and ^{244}Cm after a background correction (see Fig. 1). We obtain an estimated SF-rate of 2.3×10^{-5} per hour in sample no. 4 immediately after its preparation. Considering the uncertainties of the cross section estimations we use the conservative value of 4.6×10^{-5} per hour (i.e., twice the value given above) as an upper limit of the SF-rate. Thus, the probability to measure one SF-event within 96 h originating from contaminants is less than 0.44%. The upper limits for the probability to detect two and three SF-events are $9.6 \times 10^{-4}\%$, and $1.4 \times 10^{-6}\%$, respectively. Our measurements bolster the exceptional quality of the chemical separation of the Db/Rf containing fraction from heavy actinides.

Therefore, we conclude that there is no evidence for SF-decay attributed to heavy actinide isotopes in sample no. 4 from the chemical confirmation experiment of the 115 discovery [8–10]. The 15 SF-events observed in this experiment can be unambiguously assigned to decay products of $^{268}\text{115}$ in the Rf/Db region and, therefore, confirm the synthesis of element 115 in the nuclear fusion reaction of ^{48}Ca with ^{243}Am .

[1] Y. Oganessian, J. Phys. G: Nucl. Part. Phys. **34**, R165 (2007).
 [2] W. D. Myers and W. J. Swiatecki, Nucl. Phys. **81**, 1 (1966).
 [3] A. Sobiczewski, F. A. Gareev, and B. N. Kalinkin, Phys. Lett. **22**, 500 (1966).

[4] H. Meldner, Ark. Fys. **36**, 593 (1967).
 [5] S. G. Nilsson, C. F. Tsang, A. Sobiczewski, Z. Szymanski, S. Wycech, C. Gustafson, I.-L. Lamm, P. Moller, and B. Nilsson, Nucl. Phys. **A131**, 1 (1969).

- [6] U. Mosel and W. Greiner, *Z. Phys. A* **222**, 261 (1969).
- [7] Y. T. Oganessian, V. K. Utyonkov, Y. V. Lobanov, F. S. Abdullin, A. N. Polyakov, I. V. Shirokovsky, Y. S. Tsyganov, G. G. Gulbekian, S. L. Bogomolov, A. N. Mezentsev *et al.*, *Phys. Rev. C* **69**, 021601(R) (2004).
- [8] S. N. Dmitriev, Y. T. Oganessian, V. K. Utyonkov, S. V. Shishkin, A. V. Yeremin, Y. V. Lobanov, Y. S. Tsyganov, V. I. Chepygin, E. A. Sokol, G. F. Vostokin *et al.*, *Mendeleev Commun.* **15**, 1 (2005).
- [9] D. Schumann, H. Bruchertseifer, R. Eichler, B. Eichler, H. W. Gäggeler, S. N. Dmitriev, Y. T. Oganessian, V. P. Utyonkov, S. V. Shishkin, A. V. Yeremin *et al.*, *Radiochim. Acta* **93**, 727 (2005).
- [10] Y. T. Oganessian, V. K. Utyonkov, S. N. Dmitriev, Y. V. Lobanov, M. G. Itkis, A. N. Polyakov, Y. S. Tsyganov, A. N. Mezentsev, A. V. Yeremin, A. A. Voinov *et al.*, *Phys. Rev. C* **72**, 034611 (2005).
- [11] H. W. Schmitt, J. H. Neiler, and F. J. Walter, *Phys. Rev.* **141**, 1146 (1966).
- [12] D. Lee, H. von Gunten, B. Jacak, M. Nurmi, Y.-F. Liu, C. Luo, G. T. Seaborg, and D. C. Hoffman, *Phys. Rev. C* **25**, 286 (1982).
- [13] H. Breuer, A. C. Mignerey, V. E. Viola, K. L. Wolf, J. R. Birkelund, D. Hilscher, J. R. Huizenga, W. U. Schröder, and W. W. Wilcke, *Phys. Rev. C* **28**, 1080 (1983).
- [14] D. Lee, K. J. Moody, M. J. Nurmi, G. T. Seaborg, H. R. von Gunten, and D. C. Hoffman, *Phys. Rev. C* **27**, 2656 (1983).
- [15] S. Tanaka, K. J. Moody, and G. T. Seaborg, *Phys. Rev. C* **30**, 911 (1984).
- [16] D. C. Hoffman, M. M. Fowler, W. R. Daniels, H. R. von Gunten, D. Lee, K. J. Moody, K. Gregorich, R. Welch, G. T. Seaborg, W. Brüche *et al.*, *Phys. Rev. C* **31**, 1763 (1985).
- [17] R. B. Welch, K. J. Moody, K. E. Gregorich, D. Lee, and G. T. Seaborg, *Phys. Rev. C* **35**, 204 (1987).
- [18] K. E. Gregorich, K. J. Moody, D. Lee, W. K. Kot, R. B. Welch, P. A. Wilmarth, and G. T. Seaborg, *Phys. Rev. C* **35**, 2117 (1987).
- [19] R. M. Chasteler, R. A. Henderson, D. Lee, K. E. Gregorich, M. J. Nurmi, R. B. Welch, and D. C. Hoffman, *Phys. Rev. C* **36**, 1820 (1987).
- [20] J. D. Leyba, R. A. Henderson, H. L. Hall, C. M. Gannett, R. B. Chadwick, K. R. Czerwinski, B. A. Kadkhodayan, S. A. Kreek, G. R. Haynes, K. E. Gregorich *et al.*, *Phys. Rev. C* **41**, 2092 (1990).
- [21] J. D. Leyba, R. A. Henderson, H. L. Hall, K. R. Czerwinski, B. A. Kadkhodayan, S. A. Kreek, E. K. Brady, K. E. Gregorich, D. M. Lee, M. J. Nurmi *et al.*, *Phys. Rev. C* **44**, 1850 (1991).
- [22] H. Gäggeler, W. Brüche, M. Brügger, M. Schädel, K. Sümmerer, G. Wirth, J. V. Kratz, M. Lerch, T. Blaich, G. Herrmann *et al.*, *Phys. Rev. C* **33**, 1983 (1986).
- [23] D. G. Krige, *J. Chem. Metall. Mining Soc. S. Africa* **52**, 119 (1951).
- [24] S. Sei-Ichiro, A. Fumihiko, and Z. Masaru, *Computers and Structures* **86**, 1477 (2008).
- [25] H. Breuer, N. R. Yoder, A. C. Mignerey, V. E. Viola, K. Kwiatkowski, and K. L. Wolf, *Nucl. Instrum. Methods Phys. Res.* **204**, 419 (1983).
- [26] W. Reisdorf, J. V. Kratz, R. Bellwied, W. Brüche, H. Keller, K. Lützenkirchen, M. Schädel, K. Sümmerer, and G. Wirth, *Z. Phys. A* **342**, 411 (1992).